Abdominal Imaging

Published online: 3 July 2015

Abdom Imaging (2015) 40:2071–2090
DOI: 10.1007/s00261-015-0482-0

Diagnostic errors of right lower quadrant pain in children: beyond appendicitis

Patricia T. Chang, Gary R. Schooler, Edward Y. Lee

Department of Radiology, Boston Children's Hospital and Harvard Medical School, 300 Longwood Avenue, Boston, MA 02115, USA

Abstract

Right lower quadrant pain in children can result from various underlying conditions other than acute appendicitis. The common mimics of acute appendicitis are related to acute gastrointestinal and genitourinary diseases. Diagnosis of right lower quadrant pain in the pediatric population can be challenging, especially when the symptoms are often nonspecific. This article reviews the currently available imaging techniques for evaluating a child with right lower quadrant pain and the spectrum of differential diagnoses with a focus on imaging clues to a specific diagnosis.

Key words: Gastrointestinal—Genitourinary—Children—Appendicitis

Right lower quadrant pain is a common but often nonspecific presenting symptom in the pediatric population. Accurate diagnosis can be challenging particularly when the patient is unable to localize the pain and there are overlapping clinical symptoms, physical exam findings, and laboratory data. The most frequent cause of right lower quadrant pain requiring acute surgical intervention in the pediatric population is acute appendicitis. However, it is important to recognize that there are various other conditions that can mimic appendicitis, ranging from congenital, infectious, and neoplastic gastrointestinal causes to genitourinary causes including ovarian-related diseases, particularly in the female patient (Table 1). Clear knowledge of the spectrum of underlying causes is essential for the timely and appropriate management of pediatric patients, particularly those presenting with an acute surgical abdomen. Recognition of characteristic imaging features is important because it can guide treatment and may obviate unnecessary additional imaging evaluation or invasive procedures such as biopsy or surgery. The overarching goal of this article is to review the currently available imaging techniques for evaluating a child with right lower quadrant pain and the spectrum of differential diagnoses with a focus on imaging clues to a specific diagnosis.

Correspondence to: Edward Y. Lee; *email:* Edward.Lee@childrens.harvard.edu

Imaging technique

Imaging is an essential component in the evaluation of children with right lower quadrant pain. The appropriate use of imaging is dependent on careful initial history and physical examination. Currently available imaging modalities utilized in the assessment of children with right lower quadrant pain include radiography, ultrasound, computed tomography (CT), and magnetic resonance imaging (MRI). The primary imaging modality used at many children's institutions for the evaluation of right lower quadrant pain is ultrasound.

Plain radiographs

Plain-film abdominal radiographs are frequently used as a screening procedure in a child with a nonspecific presentation and are most useful when intestinal obstruction or perforation is a concern [1]. Chest radiographs can be obtained to exclude pneumonia, which can be a cause of abdominal pain in pediatric patients. Plain radiographs are also sometimes useful at demonstrating abnormal calcifications in the abdomen. Children with intussusception can show an abnormal bowel gas pattern on plain radiographs. In most instances, however, plain radiographs are limited in providing a specific diagnosis for right lower quadrant pain [2].

Ultrasound

Ultrasound is the preferred first-line imaging tool for right lower quadrant pain because of the lack of radiation and lower cost [3]. It not only can establish the diagnosis of appendicitis but can also aid in the diagnosis

Table 1. Spectrum of underlying conditions of right lower quadrant pain in children

Congenital
Gastrointestinal duplication cyst
Meckel's diverticulum
Urachal anomalies
Infectious
Intussusception
Parasitic infection
Colitis
Inflammatory
Crohn's disease
Ulcerative colitis
Mesenteric adenitis
Omental infarction
Henoch–Schonlein purpura
Pelvic inflammatory disease
Neoplastic
Bowel neoplasm
Ovarian neoplasm
Miscellaneous
Pyelonephritis
Renal Stone
Hemorrhagic ovarian cyst
Ovarian torsion
Endometriosis

of other abdominal and pelvic conditions that may mimic acute appendicitis. Graded compression with a linear transducer is performed to localize the appendix [3]. If the cecum is visualized but not the appendix, sagittal images may help to identify a retrocecal appendix. If the appendix is still not seen, a curved transducer should be used to evaluate deeper into the pelvis for complex free fluid or abscess formation secondary to a perforated appendix. Ultrasound evaluation is also useful in the investigation of many of the other etiologies for right lower quadrant pain, including renal disease, intussusception, and gynecologic pathology.

Computed tomography (CT)

CT can be useful in the evaluation of pediatric patients with right lower quadrant abdominal pain when there are a wide variety of diagnoses being considered, especially infectious and inflammatory bowel pathology. Intravenous contrast can improve diagnostic accuracy particularly in pediatric patients with a paucity of intraabdominal fat. The addition of oral contrast can aid in outlining intestinal pathology.

When performing CT in pediatric patients, it is important to match the beam width with the patient size in order to avoid over-irradiation. The two factors that determine the overall radiation dose are kVp and mAs, which should be carefully selected from specialized pediatric protocol charts based on patient size or age. In general, lower kVp is used for smaller patients and higher kVp for larger patients. In neonates, the kVp can be decreased to as low as 80 with adjustment of the mAs to produce acceptable and diagnostic image quality [4]. A focused CT study limited to the appropriate specific area should also be performed whenever possible in order to decrease radiation exposure.

However, given the radiation exposure to young patients with CT, magnetic resonance imaging (MRI) should be preferred to CT when available, even in the emergent setting, due to the lack of ionizing radiation.

Magnetic resonance imaging

In the past decade, MRI has increasingly been used for pediatric GI applications, including inflammatory bowel disease and appendicitis. Pediatric MRI evaluation is typically performed on a 1.5 or 3T MRI scanner with the patient in supine position, using a phased array receiver coil. Higher field strength imaging on a 3T MRI scanner offers a number of benefits for pediatric imaging, including improved signal-to-noise (SNR) and contrast-to-noise ratios (CNR), with potential for improved spatial and temporal resolution [5, 6]. However, 3T MRI also has disadvantages that can be particularly challenging for abdominal imaging, including increased susceptibility artifacts from air within bowel loops as well as increased energy deposition, which can approach patient specific absorbed ratio (SAR) limits in children. Thus, in most situations, a field strength of 1.5T is sufficient to make the majority of diagnoses in these patients.

The receiver coil for pediatric abdominal imaging should fit snugly around the pediatric patient to maximize spatial resolution and SNR. This can be challenging, because various adult MR coils need to be fitted to pediatric patients ranging from infants to adolescents. A head coil is often used for infants and small children, while a body coil is typically used for larger children and adolescents [7]. Whole body coils have also been employed with success.

Compared with adult imaging, patient motion is a more substantial problem with pediatric MRI. Sources of motion include voluntary motion from patient muscular movements in the scanner, as well as involuntary motion predominantly due to respiratory motion in children unable to suspend respiration on command. In order to minimize scan times, parallel and fast imaging techniques can be used [8].

Patient preparation

Pediatric patients over the age of 6 usually are able to cooperate with MR imaging after an explanation of the procedure and reassurance. Distraction techniques including the use of MRI-compatible music and video players, as well as scanning during off-hours to minimize ambient noise and activity can also be helpful. Similarly, newborns and young infants may tolerate MR imaging without the need for sedation, if they are well fed and comfortably swaddled. For young children under 6 years of age, conscious or deep sedation may be required in

order to relieve patient anxiety and minimize patient motion during MR imaging.

Sedation

Several sedation medications are currently used for pediatric MRI, including chloral hydrate, pentobarbital, propofol, and midazolam [9, 10]. Advantages of sedation in children who cannot tolerate MRI while awake include reduction in scan time and improvement in image quality. Generally, the least amount of sedation necessary for the pediatric patient to tolerate MRI is administered, both to minimize post-MRI side effects and to facilitate patient induction and emergence from sedation. As always, the proper balance should be maintained between adequate sedation for patient comfort and scan performance and minimization of potential neurologic and cognitive effects associated with prolonged anesthesia [11].

Intravenous contrast administration

Contrast agents used for clinical pediatric MR imaging are gadolinium chelated, extracellular contrast agents that cause T1 shortening within blood vessels and perfused tissues. The typical dose for intravenous administration is 0.1 mmol/kg [12].

Imaging sequences

The MRI sequences for evaluation of the abdomen in pediatric patients depends on the indication for the exam, but in general, they include coronal and axial fast spin echo fat-suppressed T2, axial or coronal T1, and axial/coronal fat-suppressed T1 pre- and post-contrast administration if needed (Table 2). In older children and adolescents, these MRI sequences can be performed as a 15–25 second breath hold. However, in younger children and sedated patients, these sequences need to be modified in order to account for respiratory motion and longer scan acquisition times. Such modifications include increased utilization of single shot fast spin echo sequences, respiratory triggering/navigator echoes, and signal averaging to reduce respiratory artifact [6].

Spectrum of underlying causes

Congenital conditions

Gastrointestinal duplication cyst

Gastrointestinal duplication cysts are congenital cystic or tubular anomalies of the gastrointestinal system. They are characterized by a smooth muscle wall, contiguity with and attachment to a segment of the alimentary tract, and a shared vascular supply with a portion of the native alimentary tract. Gastrointestinal duplication cysts usually do not communicate with the lumen of the native bowel and thus are most often fluid filled. Clinical presentation is usually related to their size and location of the duplication. Common abdominal manifestations include abdominal pain, vomiting, bleeding, and a palpable abdominal mass. They may act as a fulcrum for segmental volvulus [13] or as a lead point in intussusception and should be suspected when the intussusception occurs in infants within the first 3 months of life.

Table 2. Pediatric Abdominal MRI imaging techniques based on clinical indication

Indication	Sequences
Infection	Coronal fast recovery fast spin echo (FRFSE) T2 fat saturation (FS)
	Axial FRFSE T2 FS
	Axial T1
Neoplasm	Axial FRFSE T2 FS
	Coronal T1
	Coronal FRFSE T2 FS
	Axial diffusion-weighted imaging (DWI)
	Post-contrast axial T1 FS
	Post-contrast coronal T1 FS
	For ovarian neoplasms, the following sequences should be performed in place of the post-contrast axial and coronal T1 FS sequences: Axial dynamic contrast enhanced (DCE) 3D spoiled ultrafast T1/FS gradient echo of the pelvis and the same sequence in the coronal plane with a bigger field of view to explore the peritoneum
	Coronal 3D MRA gradient echo with contrast for renal tumors
Gynecologic anomalies	Sagittal fast spin echo (FSE) T2 FS
	Coronal oblique (parallel to the uterus) FSE T2 FS
	Axial oblique (perpendicular to the uterus) FSE T2 FS
	Axial FSE proton density FS (straight axials for vagina)
	Coronal T1
Inflammatory bowel disease	Coronal single shot fast spin echo (SSFSE) T2 FS
	Axial SSFSE T2 FS
	Axial balanced steady-state free precession (bSSFP)
	Coronal bSSFP peristalsis
	Coronal fast spoiled gradient echo (FSPGR) FS
	Coronal FSPGR FS post-contrast
	Axial FSPGR T1 FS post-contrast of entire abdomen

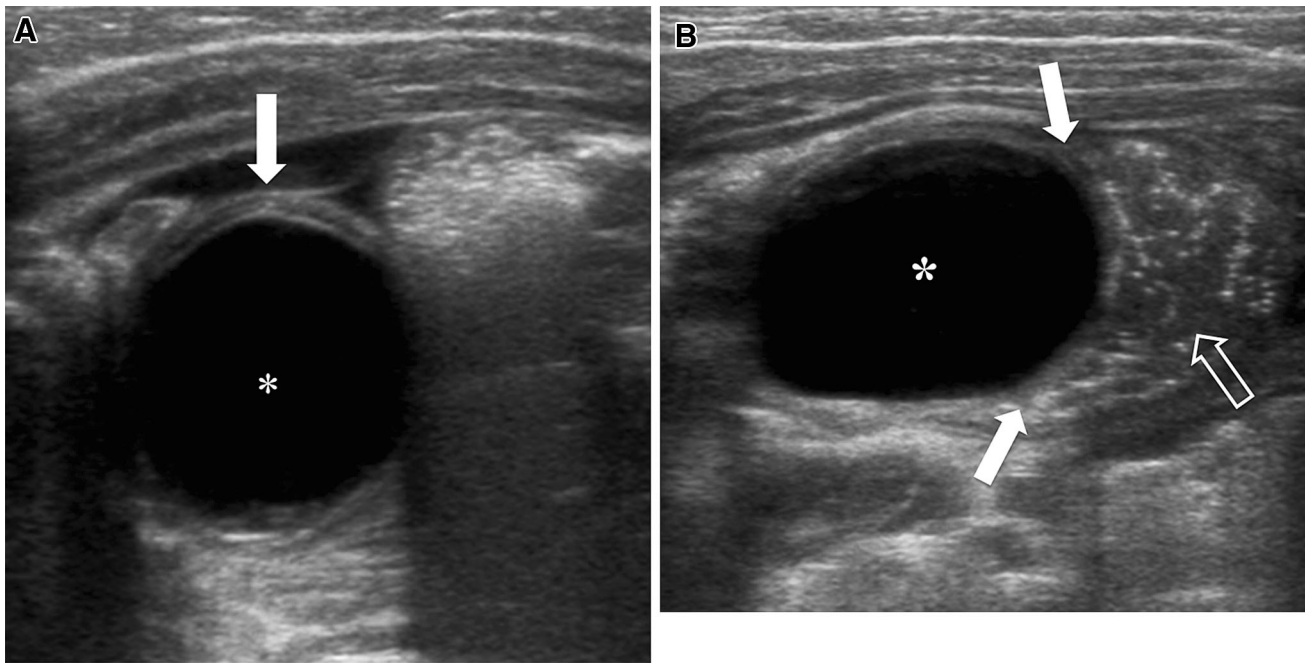

Fig. 1. Transverse (**A**) and longitudinal (**B**) ultrasound images of the right lower quadrant in an infant demonstrate a circular anechoic duplication cyst (*asterisk*). The wall exhibits alternating hyper- and hypoechoic rings typical for gut signature (*closed arrow*). Note in (**B**) the cyst sharing a common wall (*closed arrows*) with an adjacent loop of bowel containing gas and stool (*open arrow*).

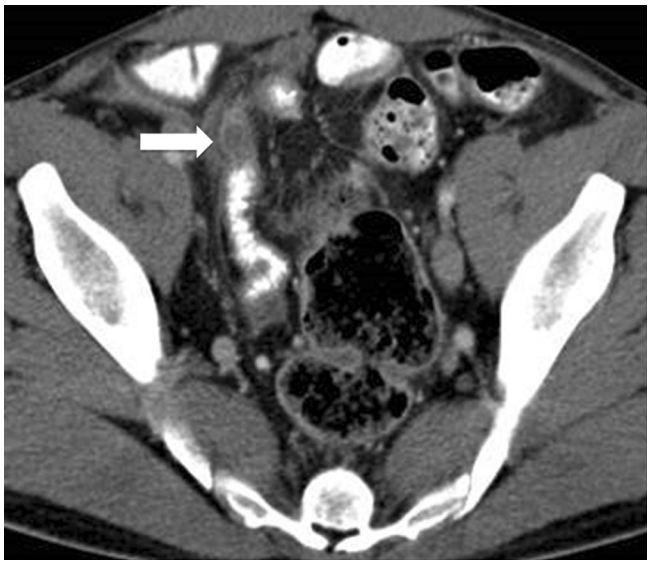

Fig. 2. Axial CT image with enteric and intravenous contrast material shows a centrally hypoattenuating and peripherally enhancing structure (*arrow*) arising from the wall of the distal ileum that was surgically proven to be a Meckel's diverticulum. Note the surrounding mesenteric fat stranding and wall thickening in the ileum indicating the presence of inflammation.

Ultrasound is the most commonly used modality in the evaluation of gastrointestinal duplication cysts. An anechoic cyst can be seen with a characteristic ultrasound appearance of "gut-signature," consisting of an echogenic inner mucosa, hypoechoic middle muscular layer, and echogenic outer serosa layer (Fig. 1). If there is inflammation, ulceration, or perforation, debris can be seen within the cyst. On CT, a fluid-filled cyst with variable contents of varying Hounsfield units will be seen typically on the mesenteric border of the involved bowel segment, often with contrast enhancement of the cyst wall. MRI will usually exhibit hypointensity on T1 and hyperintensity on T2 if the cyst is simple, but the signal intensity can vary depending on the cyst contents.

The most common treatment of duplication cysts is surgical resection in order to eliminate potential complication of local mass effect causing obstructive symptoms, surrounding inflammation, and hemorrhage. Marsupialization with internal drainage may also be also performed. Prognosis is generally excellent, but there have been rare reports of malignant transformation in unresected enteric cysts in the pediatric population [14, 15].

Meckel's diverticulum

Meckel's diverticulum is a remnant of the vitelline or omphalomesenteric duct, the embryologic communication between the embryonic gut and yolk sac. It occurs in approximately 2% of the general population. It is typically found within 2 feet of the ileocecal valve and associated with clinical symptoms in patients usually

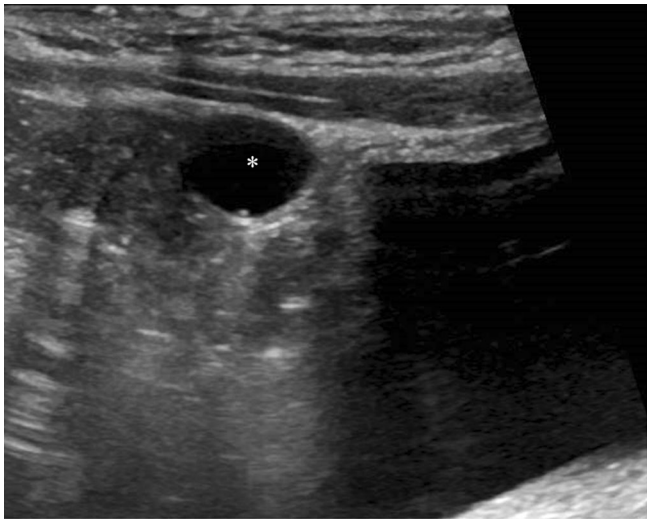

Fig. 3. Longitudinal ultrasound image in a neonate demonstrates an anechoic cyst (*asterisk*) just superior to the dome of the bladder consistent with a urachal cyst.

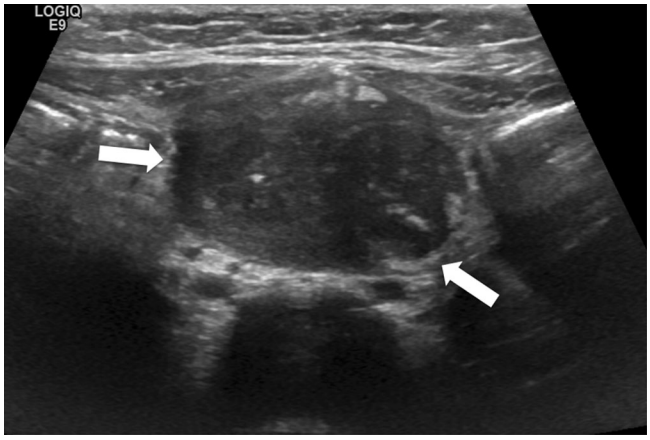

Fig. 4. Transverse ultrasound image superior to the bladder in a patient with clinical concern for umbilicus/abdominal wall cellulitis shows an elongated heterogeneous lesion (*arrows*) in the midline extending from the dome of the bladder to the umbilicus, compatible with inflammatory changes related to an underlying urachal remnant.

before 2 years of age. The most common clinical presentation is painless rectal bleeding. The incidence of gastric mucosa within bleeding Meckel's diverticula is estimated at 23%–80% [16, 17]. Heterotopic pancreatic tissue is found in 5%–16% of cases [16]. Gastric and pancreatic mucosa can also lead to inflammation of the diverticulum, with the abdominal pain mimicking appendicitis. Patients can also present with small bowel obstruction, intussusception, volvulus, or perforation.

The most specific imaging test for Meckel's diverticulum is a Tc-99m pertechnetate scan, which is dependent on the presence of gastric mucosa. The classic imaging appearance is focal tracer accumulation in the right lower quadrant and appears simultaneously with and as intensely as gastric uptake. Abdominal radiographs may be nonspecific or show a right lower quadrant mass, displacement of bowel loops, and obstruction. Ultrasound may demonstrate a thick-walled, mixed echogenicity, and tubular structure in the right lower quadrant. An inflamed Meckel's diverticulum can also present as a cyst on ultrasound, but the mucosal layers are more irregular than those typically found in an intestinal duplication. On CT, a Meckel's diverticulum can be found incidentally originating from the ileum as a blind-ending structure that may show contrast opacification. The findings of an inflamed Meckel's diverticulum can be very similar to appendicitis, with a thick-walled, blind-ending structure near the cecum associated with surrounding inflammatory changes (Fig. 2). Therefore, it is important to differentiate these entities by documenting the presence of the normal appendix. The CT findings of a small bowel obstruction caused by Meckel's diverticulum are nonspecific and similar to those resulting from other entities causing obstruction. If an intussusception cannot be reduced, a small bowel obstruction related to a Meckel's diverticulum should be considered.

The treatment of a complicated Meckel's diverticulum is surgical resection with primary closure of the small intestine. An appendectomy is also typically performed. For asymptomatic patients with Meckel's diverticulum that are incidentally discovered, treatment options are less clear, but generally they are removed given the complications that can occur if left unresected.

Urachal anomalies

Urachal anomalies are caused by the persistence of part or all of the fetal allantoic stalk, which is the connection between the bladder dome and the umbilicus. Failure of the urachus to normally regress results in one of four disorders: (1) patent urachus, (2) urachal sinus, (3) urachal diverticulum, and (4) urachal cyst. Patients can present with umbilical discharge, local infection, lower abdominal pain, and urinary tract infection.

The best primary imaging modality for assessment of possible urachal anomalies is ultrasound in the pediatric population. A structure with a thick, well-defined wall arising from the dome of the bladder will be seen and may or may not contain fluid. The size and shape of the lesion depend on the type of remnant and presence or absence of inflammation (Figs. 3, 4). A voiding cystourethrogram (VCUG) may demonstrate patency of the urachus or help to differentiate a urachal cyst from a urachal diverticulum if the ultrasound findings are not conclusive. Urachal anomalies can also be incidentally found on CT scans performed for other reasons and to further assess a complex lesion seen on ultrasound.

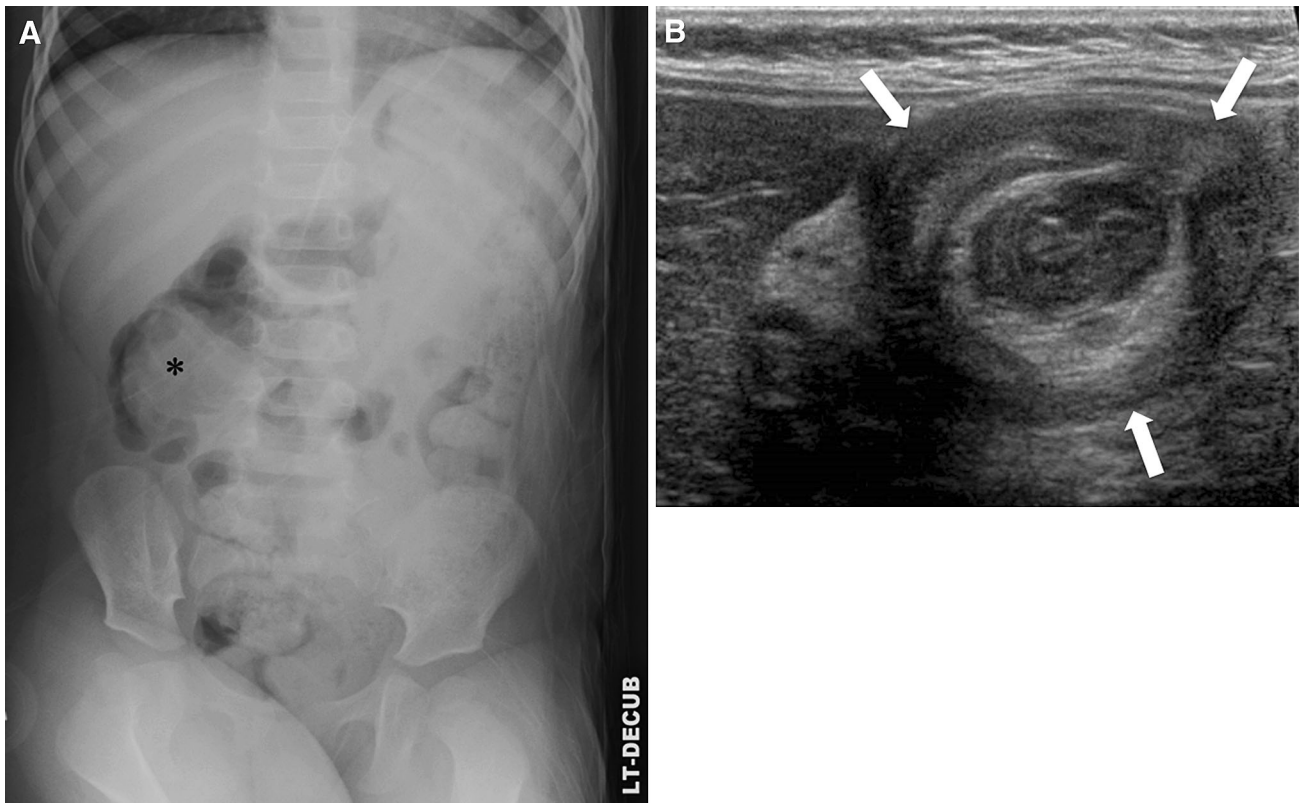

Fig. 5. Left lateral decubitus radiograph in a young child (**A**) who presented with abdominal pain demonstrates a round soft tissue density mass (*asterisk*) outlined by gas within the right hemiabdomen. Longitudinal ultrasound image of the right upper quadrant in the same patient (**B**) reveals a mass with alternating rings of hyper- and hypoechoic mesenteric fat and bowel wall consistent with an ileocolic intussusception (*arrows*).

In patients younger than 6 months, urachal remnants typically resolve with nonoperative management. Over the age of 6 months, however, surgical resection is recommended especially if symptoms persist or the urachal remnant fails to resolve. There is an increased risk of malignancy (adenocarcinoma, mucinous cystadenocarcinoma, and villous adenoma) after the fourth decade if not resected, mostly in men [18].

Infectious conditions

Intussusception

Intussusception is an acquired invagination of a segment of bowel into the adjacent distal segment. It causes bowel obstruction and edema, with ischemic changes eventually supervening due to the compression of the associated mesenteric vasculature. The majority of cases is idiopathic likely secondary to lymphoid hypertrophy and may be preceded by a viral illness. Less commonly, intussusception is triggered by a pathologic lead point (Meckel's diverticulum, duplication cyst, polyp, or lymphoma), especially when it occurs outside of the typical idiopathic age range [19, 20]. Affected pediatric patients characteristically present with a triad of vomiting, colicky intermittent often severe abdominal pain, and red currant jelly stool. Other symptoms include lethargy, diarrhea, and/or a palpable abdominal mass.

Abdominal radiographs have low sensitivity and specificity for the detection of intussusception. However, visualization of a curvilinear soft tissue mass within the colon (the crescent sign) is nearly a pathognomonic sign (Fig. 5A). Non-visualization of air-filled cecum/ascending colon is a suggestive sign of intussusception. Abdominal radiographs are also important in the assessment of intraperitoneal free air and small bowel obstruction, which can indicate bowel edema and a lower chance of non-operatively reducing the intussusception successfully.

Ultrasound has the highest sensitivity for the diagnosis of intussusception in the pediatric population. Transverse ultrasound usually demonstrates a "target" or "doughnut" appearance with a hypoechoic outer rim of homogenous thickness and a central core of intussusceptum and adjacent mesentery (Fig. 5B). A larger mass with a 3–5 cm diameter is more likely to be ileocolic or colocolic, while a smaller mass with less than a 2.5 cm diameter is likely secondary to be a small bowel-small bowel intussusception.

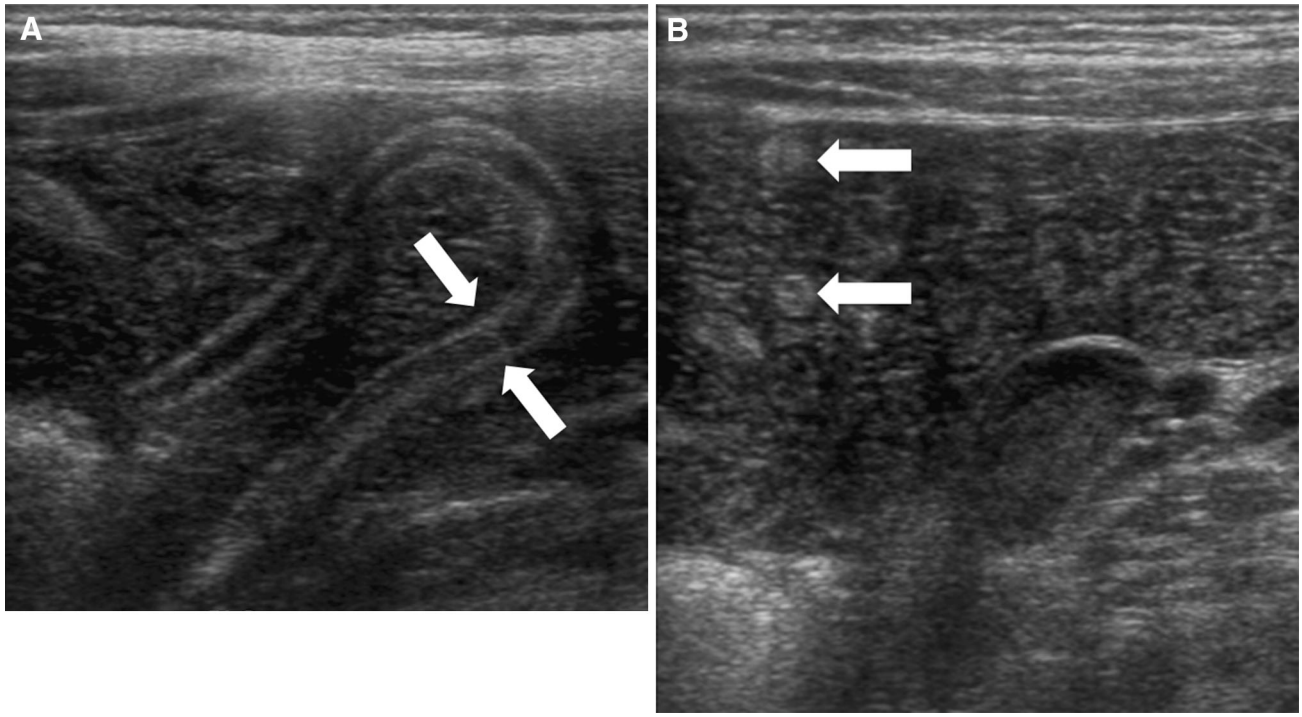

Fig. 6. Ultrasound image of a 12-year-old boy from Pakistan presenting with abdominal pain (**A**) demonstrates two long parallel curvilinear echogenic structures within the small bowel separated by a hypoechoic region (*arrows*). Transverse view (**B**) shows a target-like appearance (*arrows*). The stool ova and parasite examination revealed the presence of *Ascaris lumbricoides* ova.

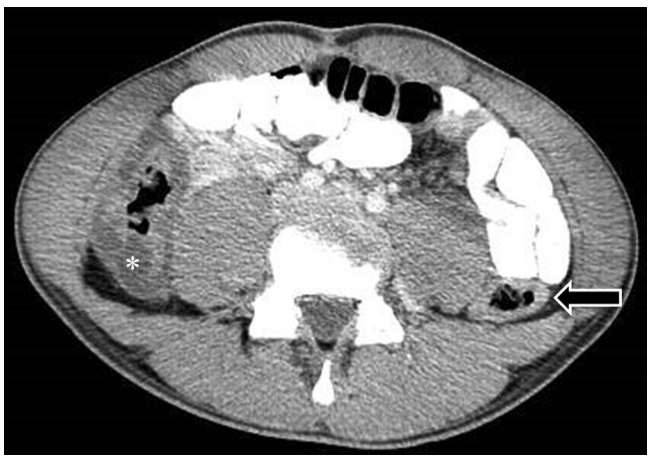

Fig. 7. Axial CT image with intravenous and enteric contrast shows thickening of the cecum/ascending colonic wall (*asterisk*) and to a lesser degree the descending colonic wall (*arrow*) in this adolescent patient with colitis.

CT and MRI are not routinely performed for suspected intussusception in children. However, CT may be the initial modality in a child presenting with nonspecific abdominal pain. A target appearance can also be seen on CT, and as with ultrasound, if an intussusception is identified, attention should be paid to potential lead points.

Enema reduction is the treatment of choice for ileocolic and colocolic intussusceptions. Surgical consultation should be obtained prior to the reduction in the event of reduction failure or when enema is contraindicated in the cases of peritonitis or pneumoperitoneum. On an air contrast enema, a round soft tissue mass within a colonic air column will be seen (meniscus sign) moving retrograde with increased pressure. Successful reduction is visualized by reflux of air into small bowel and resolution of the soft tissue mass. Recurrences are typically treated up to three times prior to considering surgical exploration for a potential pathologic lead point.

Parasitic infection

The gastrointestinal tract is the primary site of involvement by parasites during their life cycle. Although mostly endemic in underdeveloped or developing countries where sanitation is poor, parasitic infections are now more commonly encountered in developed countries because of increased immigration and traveling. Common intestinal parasitic infections include amebiasis, ascariasis, anisakiasis, strongyloidiasis, ancyclostomiasis, trichuriasis, and tapeworm disease. *Ascaris lumbricoides* is one of the most common parasitic infestations of the GI tract worldwide; giardiasis is the most common protozoal disease in the United States; and amebiasis infests 10% of the world population [21]. Common signs and

symptoms of a parasitic infection include abdominal pain, diarrhea, nausea, vomiting, weight loss, malabsorption, fever, and GI bleeding. Various parasitic infections have predilections for different locations in the body: ascariasis is typically found in the small bowel, colon, common bile duct, or pancreatic duct; giardiasis in the duodenum and jejunum; and amebiasis in the colon and liver.

Ascariasis produces linear filling defects on ultrasound and fluoroscopic imaging (Fig. 6). Giardiasis appears as thickened duodenal/jejunal folds on fluoroscopic imaging, while amebiasis can present as diffuse ulcerating colitis or as a liver abscess on CT.

Treatment regimens depend on the type of parasitic infection. Ascariasis is treated with antihelminthic chemotherapy with mebendazole, albendazole, or pyrantel pamoate. Giardiasis is treated with nitazoxanide or metronidazole, and amebiasis is treated with metronidazole.

Colitis

Infectious colitis is a major cause of childhood morbidity and death in developing countries. It can be due to bacterial, viral, fungal, or parasitic infections. Viruses are the most common cause of pediatric intestinal infection in the United States [22]. There usually is an acute onset of symptoms that include watery or bloody diarrhea, abdominal pain, fever, headache, nausea, and vomiting.

Diagnosis can usually be made with clinical presentation and lab tests, and thus imaging studies are generally not indicated for the diagnosis of infectious diarrhea in children. However, symptoms may mimic other abdominal conditions such as appendicitis or intussusception, for which imaging is requested in order to exclude these entities. Ultrasound typically shows symmetric wall thickening, dilatation, and mural hyperemia. Abscess and surrounding inflammatory changes can also be seen in complicated cases. CT and MRI may show mucosal and/or mural edematous thickening, mucosal and serosal enhancement, air-fluid levels, and perienteric fat stranding (Fig. 7).

Treatment is dependent on the underlying pathogen. Viral and bacterial gastroenteritis are usually self-limiting with supportive rehydration therapies. Antihelminthic drugs can be given for parasitic infections, and agents such as metronidazole and nitazoxanide are active against certain fungal infections. Prognosis is generally good with treatment, but complications can occur, such as hemorrhage, perforation, obstruction, and toxic megacolon.

Inflammatory conditions

Crohn's disease

Crohn's disease is one of two major disorders that comprises inflammatory bowel disease (IBD), the other being ulcerative colitis. Crohn's disease typically peaks in the second and third decades but up to a quarter of patients present during childhood or adolescence [23]. It may involve any portion of the GI tract and is characterized by segmental transmural granulomatous inflammation of the intestine. The disease most commonly

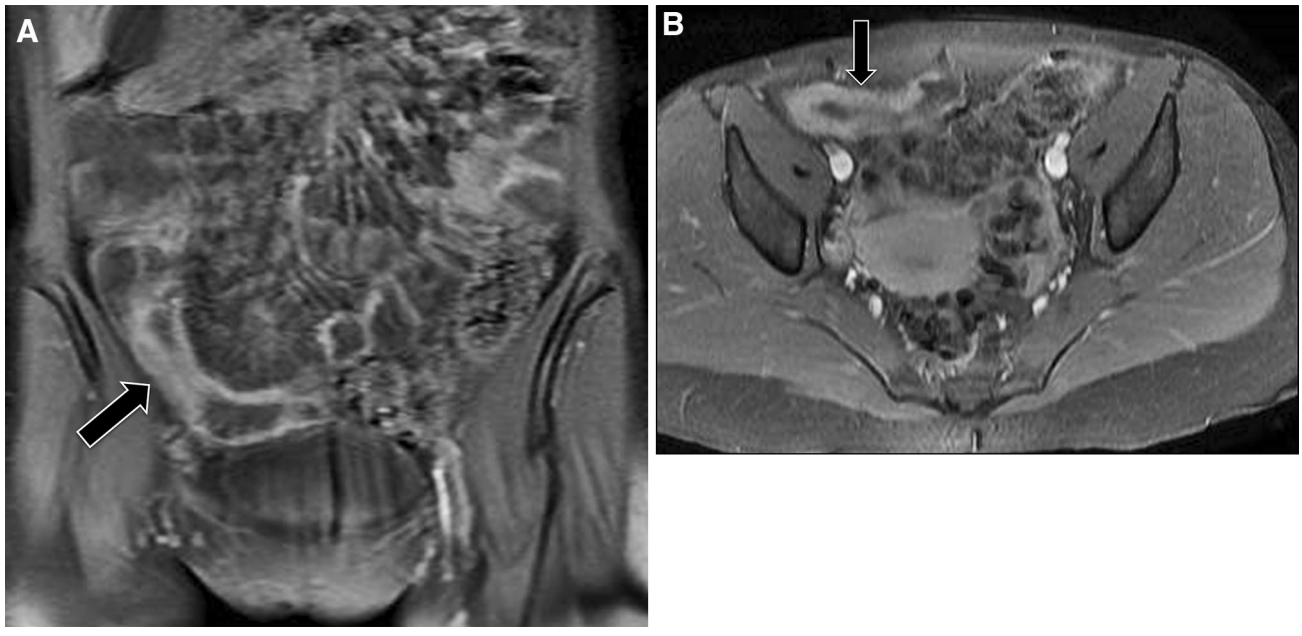

Fig. 8. Coronal (**A**) and axial (**B**) post-contrast T1 weighted fat-saturated MRI images of the lower abdomen and pelvis show wall thickening and hyperenhancement of the terminal ileum in the right lower quadrant (*arrow*), consistent with the diagnosis of Crohn's disease.

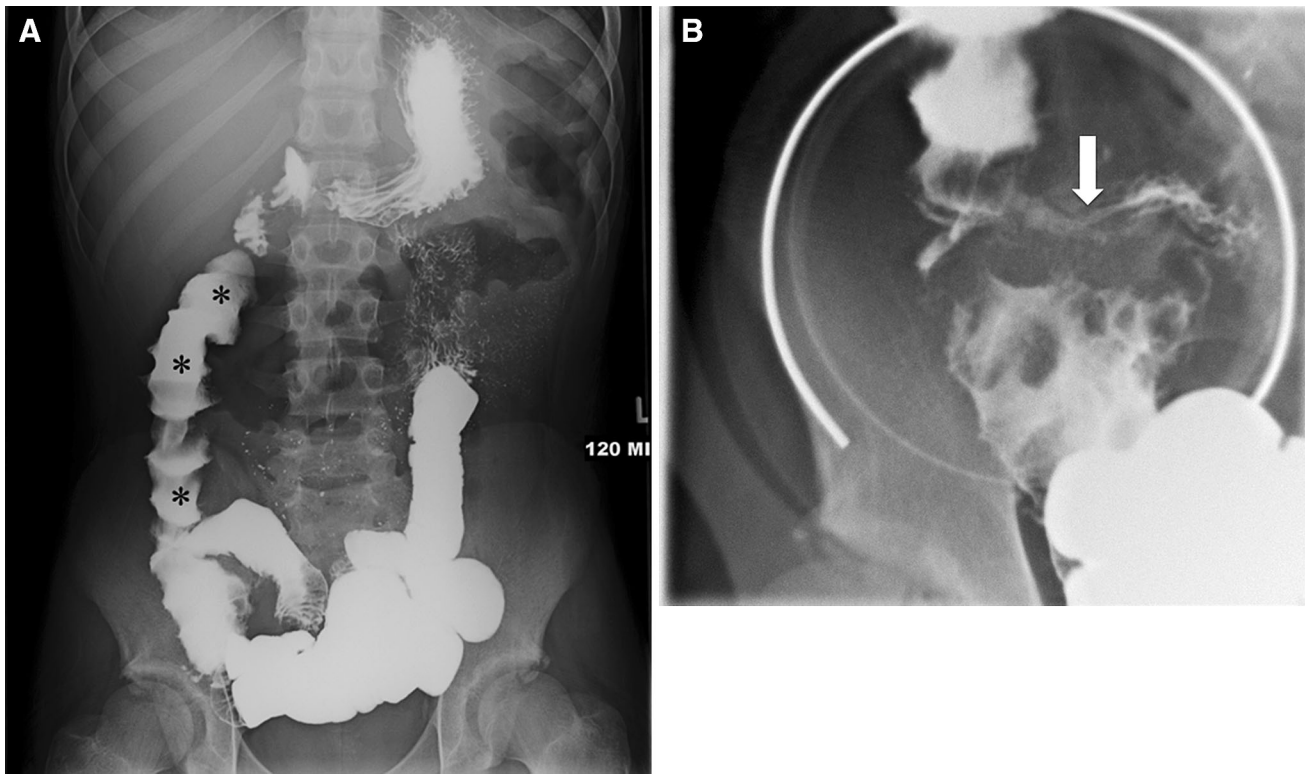

Fig. 9. Small bowel follow-through study (**A**) shows a featureless and edematous ascending colon with decreased luminal diameter (*asterisk*). Spot compression view (**B**) of the terminal ileum shows focal narrowing (*arrow*) of the terminal ileum at the ileocecal junction, compatible with backwash ileitis.

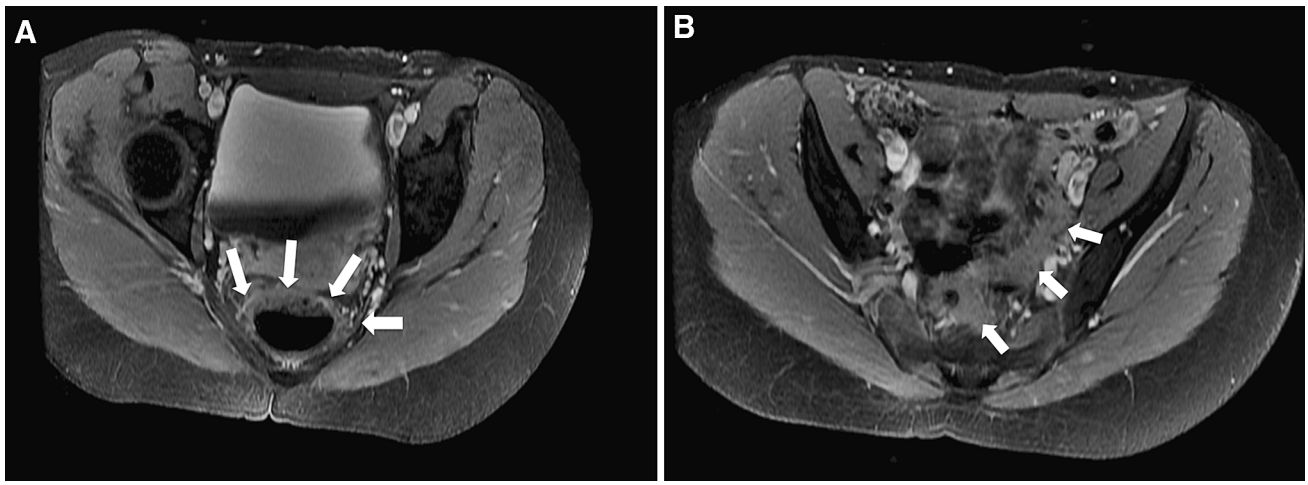

Fig. 10. Axial post-contrast T1 images with fat-suppression show mucosal enhancement of the rectum (*arrows*) (**A**) and sigmoid colon (**B**) with mild associated mucosal thickening (*arrows*).

occurs in the ileum and cecum, but the disease can occur anywhere along the GI tract from the mouth to the anus and may occur without terminal ileal involvement.

Clinical presentation is variable. Constitutional signs and symptoms include diarrhea, abdominal pain, anorexia, and weight loss. Some pediatric patients have symptoms that manifest acutely with right lower quadrant pain and fever, mimicking appendicitis. Extraintestinal symptoms can also occur, including fever, aphthous stomatitis, arthralgias, arthritis, sacroilliitis, erythema nodosum, and digital clubbing. The most common extraintestinal manifestation in children with Crohn's disease is arthritis.

Radiographs, ultrasound, fluoroscopy, CT, and MRI can all be used to evaluate pediatric patients with sus-

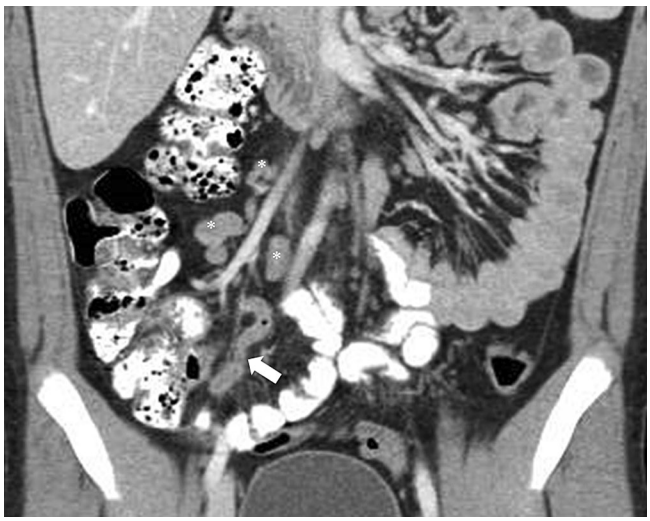

Fig. 11. Coronal image from a CT scan with intravenous and enteric contrast in a pediatric patient with right lower quadrant pain shows multiple enlarged right lower quadrant mesenteric lymph nodes (*asterisk*). Note the normal appendix (*arrow*).

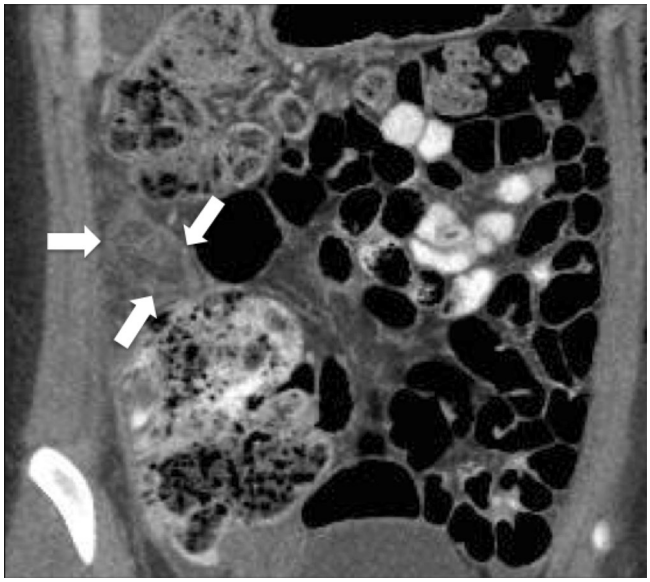

Fig. 12. Coronal CT image with intravenous and enteric contrast shows a poorly defined fatty mass (*arrows*) within the right hemiabdomen with reticulation of the surrounding fat consistent with an omental infarction.

pected Crohn's disease. However, the diagnosis is ultimately made by endoscopic and/or histologic criteria. On radiographs, bowel wall edema manifesting as "thumbprinting" can be seen. Other complications of Crohn's disease can also be visualized, including ileus and obstruction. Fluoroscopy may show skip lesions due to segmental involvement, aphthous ulcers, distortion of fold pattern, strictures, fistulae, and pseudodiverticulae. On ultrasound, segmental bowel wall thickening and hyperemia can be seen along with surrounding inflammatory changes and sometimes abscess formation. CT and MRI are useful in the evaluation of disease activity and its complications. CT and MR enterography can identify intraperitoneal complications such as fistulae and abscesses as well as the extent of intestinal involvement. MR enterography is being utilized more in pediatric centers than CT enterography due to the lack of ionizing radiation (Fig. 8). In addition, MR enterography can differentiate active inflammation from chronic disease. MR enterography is also superior to CT enterography in the evaluation of perianal fistulae.

Initial medical therapy to suppress inflammation includes steroids and immunosuppressants. Most pediatric patients with Crohn's disease, however, eventually need surgical resection of diseased bowel.

Ulcerative colitis

Ulcerative colitis is an idiopathic inflammatory bowel disease that primarily involves the colon in contrast to Crohn's disease. It typically affects older children and young adults. Ulcerative colitis is primarily a mucosal disease that begins at the rectum in the majority of cases. Unlike Crohn's disease, transmural involvement is uncommon and skip lesions are uncharacteristic. Most affected pediatric patients present with progressive chronic diarrhea. Toxic megacolon can sometimes be seen, primarily involving the transverse colon. Extraintestinal involvement is variable in children and includes arthritis, skin involvement, uveitis, digital clubbing, stomal ulcers, primary sclerosing cholangitis, and autoimmune hepatitis.

As in Crohn's disease, radiographs are often nonspecific and may show thumb-printing. If there is toxic megacolon, the affected children should not undergo a contrast enema due to the increased risk of perforation. Contrast enema may show colorectal narrowing with fine granularity and "collar button" ulcers. Submucosal fibrosis can lead to a "lead pipe" colon, which is stiff, shortened, and tubular (Fig. 9A). The terminal ileum may become secondarily affected when there is proximal colonic involvement from backwash ileitis (Fig. 9A). As in Crohn's disease, CT and MRI can be performed to evaluate disease activity and complications. Mucosal hyperenhancement with colonic/rectal wall thickening can be seen (Fig. 10). Pre-sacral thickening and a widened presacral space can be seen in late-stage disease.

Treatment for ulcerative colitis is similar to that for Crohn's disease with medical therapy and surgical resection of diseased bowel. Patients with long-term ulcerative colitis have an increased risk of colonic carcinomas.

Mesenteric adenitis

Mesenteric adenitis is a self-limiting inflammatory process that affects the mesenteric lymph nodes in the right

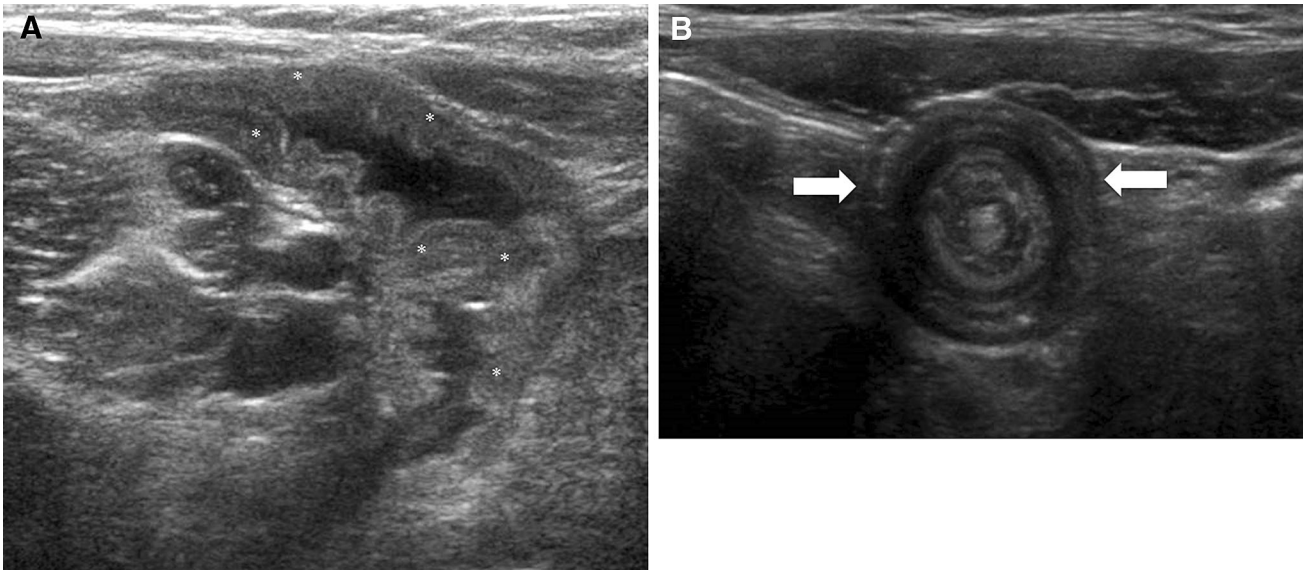

Fig. 13. Transverse ultrasound image of the right lower quadrant (**A**) demonstrates wall thickening of a loop of distal small bowel (*asterisk*) in a pediatric patient with the characteristic purpuric rash and a clinical diagnosis of Henoch-Schonlein purpura. Another transverse ultrasound image in the same child obtained slightly cephalad in the abdomen (**B**) reveals a small bowel-small bowel intussusception (*arrows*) characterized by the presence of multiple alternating hyper- and hypoechoic rings of bowel wall and echogenic mesenteric fat.

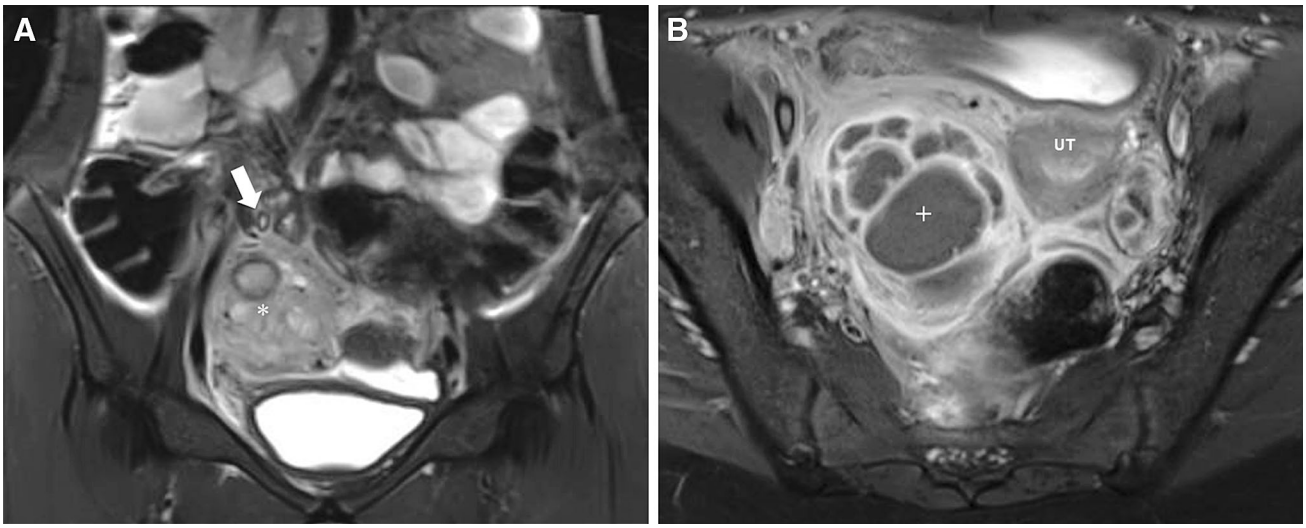

Fig. 14. Coronal T2 fat-saturated MRI image in an adolescent female (**A**) reveals a heterogeneously intense mass (*asterisk*) within the right lower quadrant, residing just superior to the bladder. Note the partially visualized normal caliber appendix just cephalad (*arrow*). Axial T1 post-contrast fat-saturated MRI image (**B**) shows a large multiloculated rim enhancing mass (+) within the right hemipelvis that displaces the uterus (UT) and is associated with exuberant surrounding abnormal enhancement, consistent with an abscess in this patient with pelvic inflammatory disease.

lower quadrant. It is often clinically mistaken for acute appendicitis and is a diagnosis of exclusion. It is typically caused by a viral agent, but other pathogens have been implicated, including *Yersinia enterocolitica*, *Helicobacter jejuni*, *Campylobacter jejuni*, and *Salmonella* or *Shigella species*. Clinical presentation is similar to that of acute appendicitis, including diffuse or focal right lower quadrant tenderness and pain with or without rebound, nausea, vomiting, diarrhea, and leukocytosis.

As with acute appendicitis, ultrasound is the current imaging modality of choice. Imaging features include a cluster of 3 or more enlarged lymph nodes in the right lower quadrant, measuring 5 mm or more in short-axis (Fig. 11). A normal appendix should be present. Associated ileal or ileocecal wall thickening can be seen.

Treatment is conservative as the condition is self-limiting with resolution of symptoms typically by 2 weeks.

Omental infarction

Omental infarction is a rare cause of acute abdominal pain in children. The majority of cases of omental infarction occur in adults. It results from vascular occlusion and segmental infarction of the greater omentum. Affected pediatric patients usually present with sudden onset of abdominal pain and localized tenderness, which given its clinical manifestations, is often mistaken for acute appendicitis. The classic location is in the right lower quadrant due to the tenuous arterial supply to the greater omentum in this region.

Ultrasound and CT are the primary modalities used for the evaluation of omental infarction. Both ultrasound and CT will show a focal triangular soft tissue mass characteristically between the anterior abdominal wall and the transverse or ascending colon. It usually appears as an area of increased echogenicity on ultrasound and increased hazy density on CT (Fig. 12).

Many surgeons believe that laparoscopic excision of omental infarction is the treatment of choice, providing rapid resolution of symptoms and decreased complications [24].

Henoch–Schonlein purpura

Henoch–Schonlein purpura (HSP) is a nonthrombocytopenic vasculitis that typically affects the bowel, skin, joints, and kidneys. It is the most common vasculitis of childhood with a prevalence peak in children 5 years of age. The clinical diagnosis is based on the triad of palpable purpuric rash along the extensor surfaces with a predilection for the lower extremities, arthralgias, and abdominal pain. Other GI symptoms include nausea, vomiting, postprandial bowel angina, and hematochezia. Arthralgias and GI symptoms may precede the characteristic rash [25], which may lead to a less directed workup. Involvement of the kidneys occurs in about half of affected patients with varying severity. Bleeding into the small bowel wall can occur, which can lead to enteroenteric intussusceptions, which most often reduce spontaneously.

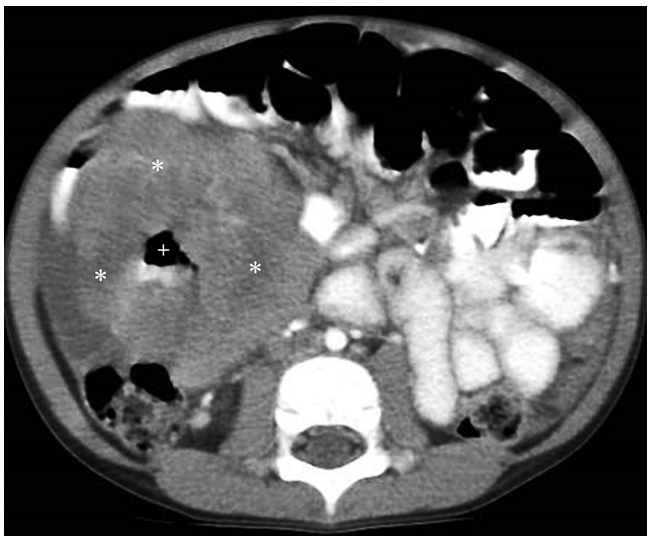

Fig. 15. Axial CT image with intravenous and enteric contrast in a young child demonstrates a large minimally enhancing mass (*asterisk*) within the right hemiabdomen. The mass resides anterior to the ascending colon and exhibits central gas and layering contrast indicating a communication with the bowel lumen (+). Biopsy of the mass ultimately revealed Burkitt lymphoma.

Findings on cross-sectional imaging include bowel wall thickening, dilation, and mesenteric edema (Fig. 13A). Small bowel-small bowel intussusceptions can also been seen (Fig. 13B). Fluoroscopic contrast studies may show segmental bowel dilation, stenosis or obstruction, bowel wall thickening with loss of mucosal fold pattern and separation of bowel loops, and intraluminal filling defects. Strictures may occur as a late sequela of the disease.

HSP usually does not require more than supportive medical treatment. However, cytotoxic/immunosuppressive therapy may be beneficial to prevent complications.

Pelvic inflammatory disease

Pelvic inflammatory disease (PID) is a spectrum of abnormalities associated with ascending spread of infection of the upper female genital tract from sexually transmitted disease. *Neisseria gonorrhoeae* and *Chlamydia trachomatis* are the most common etiologic agents. Affected patients may present with lower abdominal/pelvic pain, purulent vaginal discharge, fever, leukocytosis, and an elevated erythrocyte sedimentation rate (ESR). Other hallmark clinical symptoms include adnexal tenderness, usually bilateral, and cervical motion tenderness on bimanual examination.

Diagnosis can usually be made clinically. Imaging features are often nonspecific, but the primary goal of imaging is to evaluate for complications and potential treatment planning. Imaging may be normal in early or uncomplicated PID. In cases of salpingooophoritis, prominent ovaries may be seen adherent to the uterus. Hydrosalpinx, pyosalpinx, and tubo-ovarian abscess can be seen in more complicated cases (Fig. 14). Soft tissue stranding and infiltration of pelvic floor fascial planes can also be seen.

For uncomplicated PID, patients can be treated with antibiotics. In complicated cases, percutaneous or surgical drainage of abscesses may be required.

Neoplastic conditions

Bowel neoplasm

Neoplasms of the colon are rare in children. Most are benign juvenile polyps, which are the most common

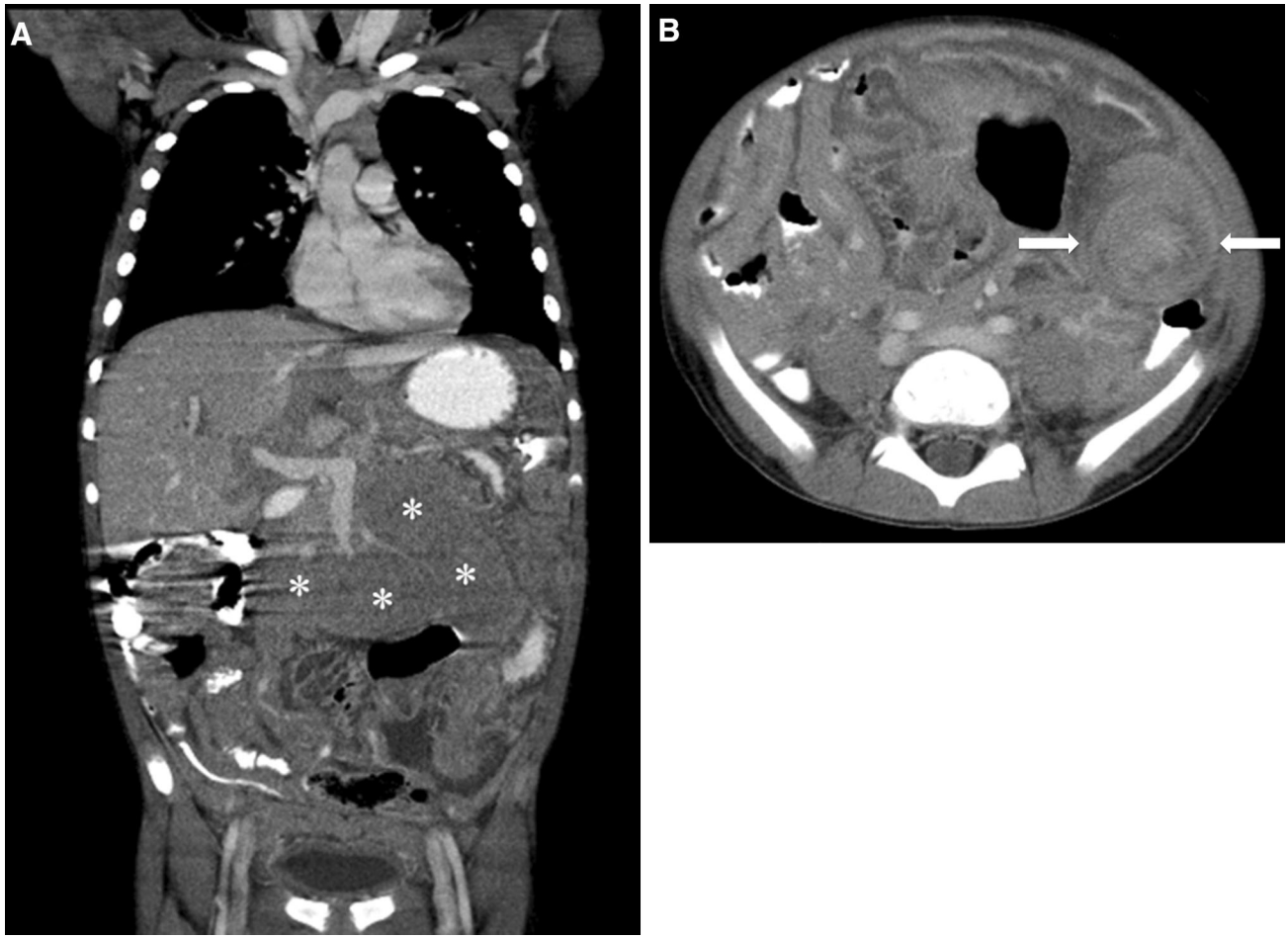

Fig. 16. Coronal CT image with intravenous and oral contrast (**A**) shows multiple large, solid, and confluent soft tissue masses (*asterisk*) in the abdomen with mass effect on the adjacent vascular structures and abdominal viscera. Axial CT image (**B**) in the same patient demonstrates abnormal appearance of the small bowel with diffuse small bowel wall thickening and edema as well as a small bowel-small bowel intussusception (*arrows*) in the left lower quadrant.

polypoid lesions in the colon in the pediatric age group. Intestinal polyposis syndromes are rare entities that can be classified as hereditary or nonhereditary. Polyps associated with the hereditary polyposis syndromes are very rare, and there usually is a known family history. Primary malignancies arising from the colon and metastatic disease to the colon are even rarer in the pediatric population.

In familial juvenile polyposis syndrome (FJP), hamartomatous polyps can affect the entire GI tract. This condition usually presents in childhood, unlike the adult onset of syndromes with adenomatous polyps. Patients with FJP have an increased risk of developing adenocarcinoma in the stomach, as well as colorectal cancer. In about 20% of affected patients, germ line mutations involved in transforming growth factor β signaling have been identified. Barium enema or MRI demonstrates multiple pedunculated filling defects.

Most affected patients with polyps detected by barium enema should undergo colonoscopy in order to excise the polyp and search for additional neoplasms. Repeat colonoscopy should be performed in 3 years for pediatric patients at high risk for developing metachronous advanced adenomas. Colonoscopic surveillance should be considered for first-degree relatives of patients with adenomatous polyps.

Lymphomas of the GI tract are the most common type of primary extranodal lymphomas. Most GI lymphomas are located in the stomach, with much fewer appearing in the small bowel, colon, and rectum. The most common signs and symptoms of lymphoma in pediatric patients include abdominal pain, weight loss, palpable mass, malabsorption, and diarrhea. Some affected pediatric patients are asymptomatic, while others may present with an acute abdomen due to obstruction or perforation.

The most common appearance of pediatric GI lymphoma on CT is an infiltrating form, which produces a circumferential, sausage-shaped mass, or aneurysmal dilatation on the antimesenteric border. Other intestinal

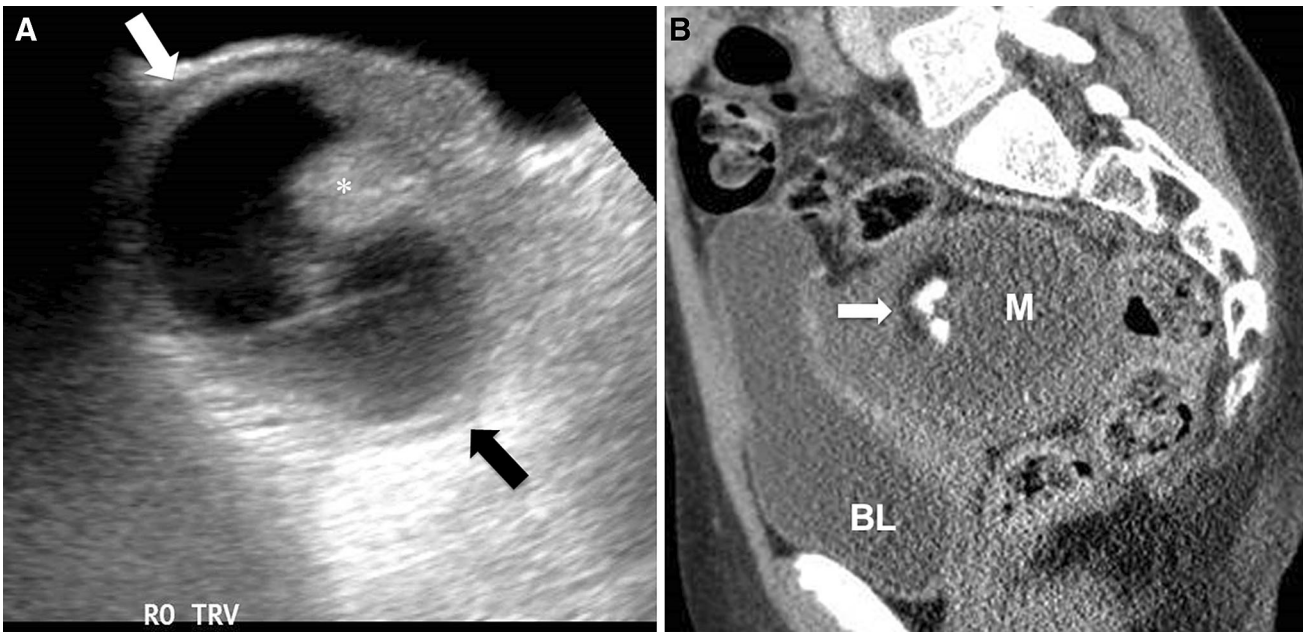

Fig. 17. Transverse ultrasound image of the right adnexa (**A**) in a young female patient presenting with right lower quadrant pain shows a solid and cystic mass (*arrows*) with an echogenic mural nodule (*asterisk*). Sagittal CT image through the pelvis (**B**) demonstrates a mass (M) within the right hemipelvis posterior to the bladder (BL) with a small focus of internal fat and calcific density (*arrow*) consistent with an ovarian teratoma.

manifestations of childhood lymphoma include a polypoid form producing a "target" lesion and a mesenteric form that appears as multiple round masses encasing mesenteric vessels; a larger, lobulated heterogeneous mass with areas of necrosis displacing small bowel loops; or as ill-defined mesenteric fat infiltration (Fig. 15). Intestinal lymphoma can also lead to intussusception due to abnormal bowel motility, particularly in the pediatric population (Fig. 16).

Treatment of intestinal lymphoma involves chemotherapy. Surgical resection is reserved for patients with lesions complicated by bleeding or perforation.

Ovarian neoplasm

Ovarian tumors in the pediatric age group are rare but can be fulminant if treated inadequately. Mature ovarian teratomas and dysgerminomas are the most common pediatric ovarian neoplasm. They generally present in postpubertal girls as a result of pain, increasing abdominal girth, and symptoms derived from hormonal effects when masses are functional. Mature teratomas are cystic tumors that contain tissue from all three germ cell layers—endoderm, mesoderm, and ectoderm. Almost all teratomas are benign, with malignancy found in less than 10% of cases.

Visualization of fat or calcification in the lesion on CT or MRI is diagnostic. Characteristic ultrasound findings of ovarian neoplasm include a cystic adnexal mass containing a shadowing echogenic nodule (dermoid plug), linear interfaces representing hair (dermoid mesh), and coarse shadowing calcification (Fig. 17).

Some teratomas contain immature elements and have the potential for metastasis as well as recurrence. Infants can present with this type and may manifest in peritoneal spread of disease. Surgical resection with conservation of part of the ovary is performed for uncomplicated cases.

Dysgerminoma is the most common malignant ovarian neoplasm in children, but it is considered low-grade. It is the ovarian counterpart of seminoma of the testis. These tumors are often large when diagnosed and usually are solid, smooth, and well encapsulated. Pure dysgerminomas are hormonally inert, but endocrine hormone secretion may be seen with germinomas that contain islands of other germ cell tumors.

On imaging, it is often visualized as a multilobulated adnexal mass with prominent fibrovascular septae (Fig. 18). Calcifications may also be present. MR is the imaging modality of choice for tumor characterization.

Dysgerminomas are very radiosensitive, and there is a generally good prognosis with treatment.

Miscellaneous

Pyelonephritis

Pyelonephritis is an acute infection of the renal parenchyma and its pelvic urothelial lining. There are different types of pyelonephritis, including acute, chronic, emphysematous, and xanthogranulomatous pyelonephritis. Clinical symp-

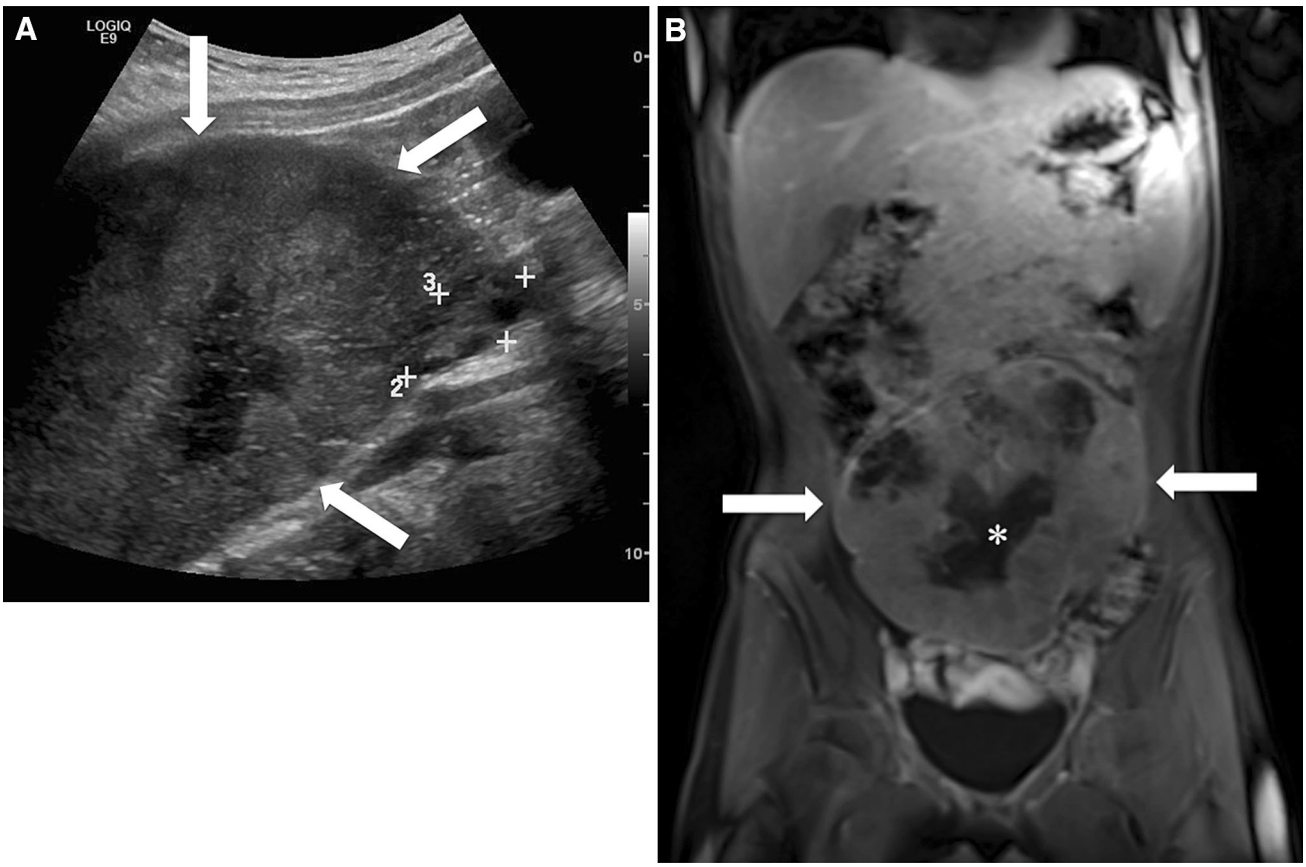

Fig. 18. Ultrasound image of the right adnexa in a 12-year-old girl (**A**) shows a large solid mass (*arrows*) associated with the right ovary (+). The mass has a thick and relatively homogeneous rind of tissue surrounding the more hypoechoic central region. Coronal MRI image with intravenous contrast (**B**) demonstrates that the solid mass (*arrows*) is heterogenous with a central area of necrosis (*asterisk*). Biopsy confirmed the mass to be a dysgerminoma.

toms in pediatric patients with pyelonephritis are nonspecific and include high fever, irritability, nausea, vomiting, flank, or abdominal pain, and hematuria. Older children are more likely to present with lower tract signs such as low-grade fever, dysuria, frequency, and suprapubic pain.

On ultrasound, poor corticomedullary differentiation can be seen with focal areas of increased or decreased echogenicity and zonal decreased perfusion of the infected renal parenchyma on color Doppler. The sensitivity of CT is similar to renal cortical scintigraphy for the diagnosis of acute pyelonephritis. The infected areas of renal parenchyma have striated or wedge-shaped areas of decreased contrast enhancement on CT (Fig. 19). A parenchymal or perinephric abscess may also be seen.

Longer and more intense antibiotic therapy is recommended for affected patients with upper urinary tracts infections than for those with infection confined to the bladder. Timely recognition and treatment are essential to prevent long-term consequences of irreversible scarring, hypertension, and chronic renal failure particularly in young children because of the increased risk of renal damage in children less than 2 years of age.

Renal stone

Renal stones can occur anywhere along the urinary tract but are usually seen in 1 of 3 locations: the renal collecting system, ureteropelvic junction (UPJ), or ureterovesicular junction (UVJ). The majority of pediatric patients with renal stones have a known predisposing condition, such as hypercalciuria, urinary stasis, or chronic infection. Renal stones are also common in patients with a urinary tract infection. Affected children often present with pain that is localized to the abdomen or the flank. Other clinical manifestations include hematuria, a common presenting symptom, urgency, dysuria, frequency, fever, pyuria, and bacteruria.

Non-contrast enhanced CT is the most sensitive imaging modality for the detection of renal stones. A calcified density is often seen in the urinary system, which can cause obstruction. Furthermore today, new imaging techniques, such as dual energy CT, facilitate the identification of uric acid stones, which can be dissolved by oral chemolysis, and extracorporeal shockwave lithotripsy (ESWL)-resistant stones, thereby potentiating the selection of the best therapeutic option for the patient

[26, 27]. Stones on ultrasound will appear as echogenic foci with demonstration of posterior acoustic shadowing and/or twinkle artifact (Fig. 20).

Most stones less than 5 mm in size likely pass spontaneously, and thus patients are treated with expectant management. If there is an underlying cause for developing renal stone, additional medical management may be needed. Surgical management with extracorporeal shock wave lithotripsy, ureteroscopy, or percutaneous nephrolithotomy can be performed for larger stones or more complex cases.

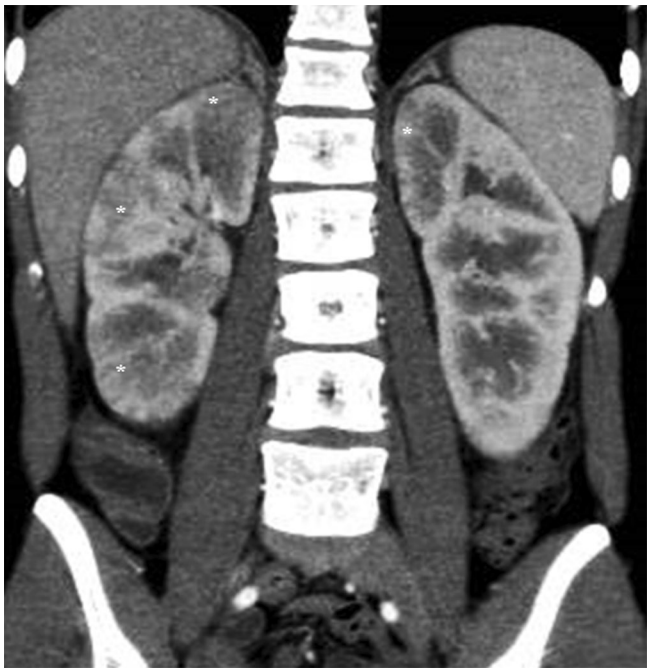

Fig. 19. Coronal CT image with intravenous contrast in an adolescent patient with right flank pain and pyelonephritis reveals patchy areas of hypoenhancement within the renal cortices (*asterisk*) of the right greater then left kidneys.

Hemorrhagic ovarian cyst

Hemorrhagic ovarian cysts usually result from hemorrhage into a corpus luteum cyst or other functional cyst when the theca interna vessels rupture into the cyst cavity. Affected patients typically present with either severe acute pelvic pain that resolves within hours or lower abdominal pain with a palpable mass on pelvic examination.

They can have a variable appearance on ultrasound depending on the stage of evolution of the clot. Typically, they have lace-like reticular echoes or an intracystic solid clot with no demonstration of internal blood flow (Fig. 21A). On pelvic MRI, the signal characteristic depends on the age of the hemorrhage (Fig. 21B).

The majority of hemorrhagic cysts resolve spontaneously over two menstrual cycles. Thus, treatment is usually supportive. If there is a history of recurrence, ovulation suppression can be considered.

Ovarian torsion

Ovarian torsion refers to partial or complete twisting of the ovarian vascular pedicle. It results in a compromise of first lymphatic, then venous, then arterial blood supply and leading to hemorrhagic infarction. Ovarian torsion can occur in either anatomically normal ovaries or in ovaries with an associated ovarian or paraovarian mass or neoplasm. Affected pediatric patients classically present with sudden onset of pelvic pain that may be

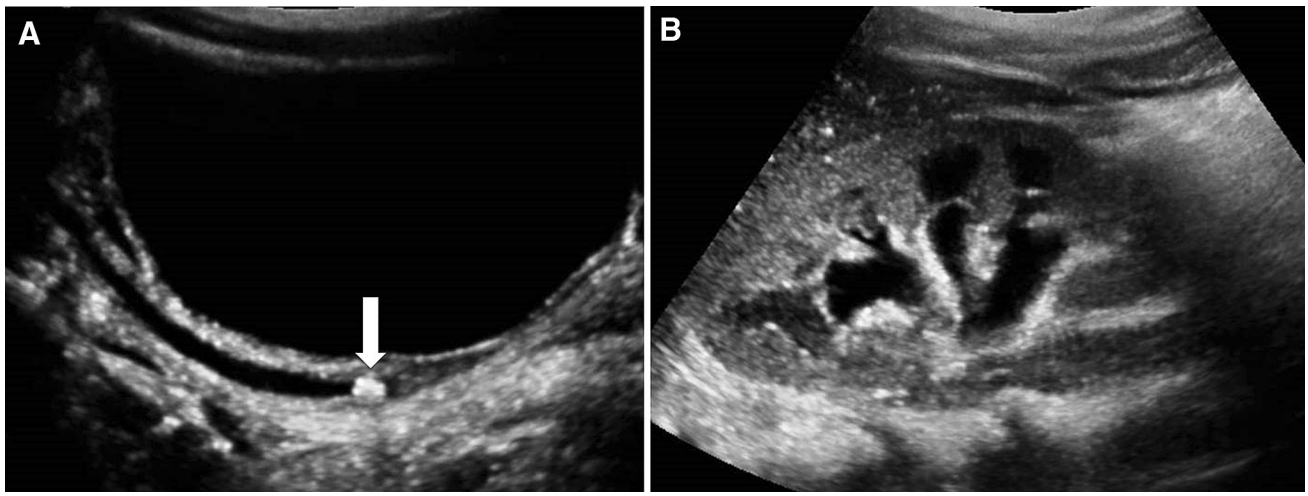

Fig. 20. Longitudinal ultrasound image through the pelvis (**A**) in an adolescent male with right flank pain shows a round, hyperechoic mass (*arrow*) within the distal ureter just proximal to the ureterovesicular junction that produces minimal posterior shadowing consistent with a ureteral calculus. Another longitudinal ultrasound image of the right kidney in the same patient (**B**) reveals mild right-sided hydronephrosis as a result of the distal ureteral calculus.

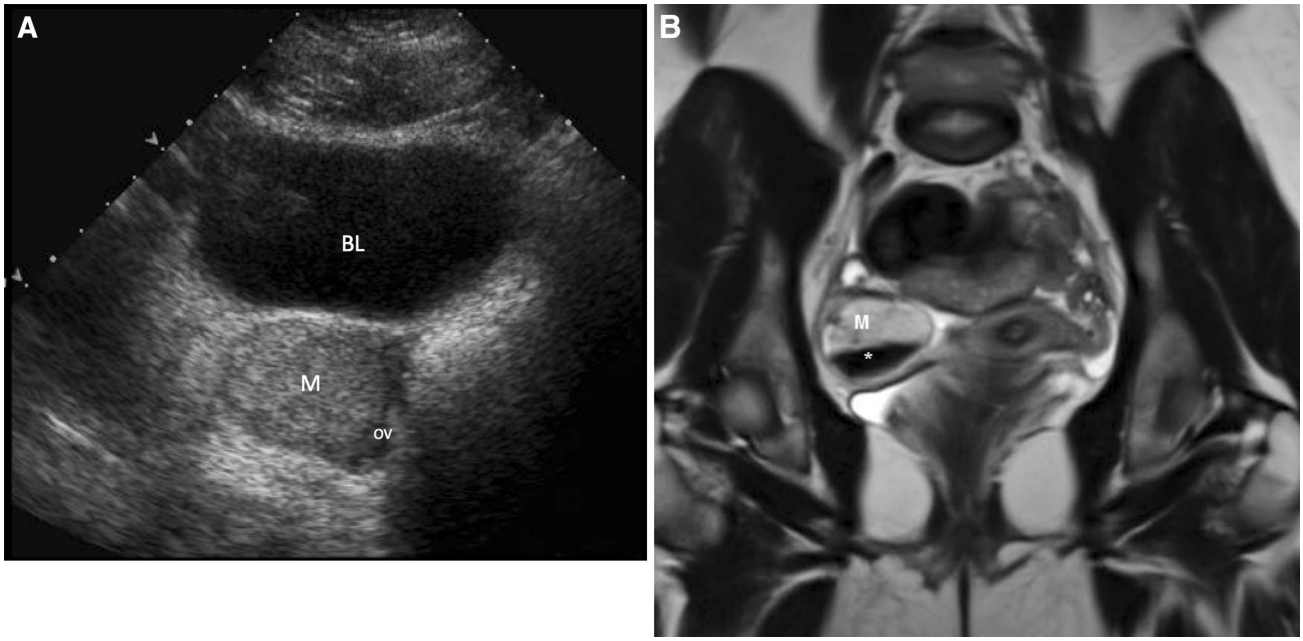

Fig. 21. Transverse ultrasound image (**A**) through the pelvis in an adolescent female demonstrates a homogeneous mildly hyperechoic mass (M) with right ovarian parenchyma around the periphery (ov). The bladder (BL) is seen anteriorly. Coronal T2-weighted MRI image of the pelvis (**B**) reveals that the right ovarian mass (M) has an internal fluid-fluid level with layering low T2 signal consistent with blood products (*asterisk*), indicating a hemorrhagic cyst.

associated with nausea, vomiting, or constipation, which may confuse the clinical picture. Leukocytosis with a left shift can also occur.

Pelvic ultrasound is the imaging modality of choice in the evaluation of ovarian torsion. The ultrasound should include both gray-scale and Doppler interrogation of the ovaries, with the gray-scale findings being the most important in making a diagnosis of ovarian torsion. The most important criterion for the diagnosis of ovarian torsion is ovarian size. The torsed ovary is larger in size compared to the normal contralateral ovary with an average adnexal ratio of 12–15 times. There can be displacement of ovarian follicles to the periphery by edema of the torsed ovary, and fluid-debris levels may be present in the follicles. The enlarged adnexa may be midline in position, often behind the uterus (Fig. 22).

The treatment of choice is a conservative surgical approach with ovarian detorsion and if necessary, removal of the mass causing the torsion. Postoperative follow-up ultrasound may be used to assess the recovery of an ovary post torsion and surgical treatment.

Endometriosis

Endometriosis is the presence of ectopic endometrial glands and stroma outside the endometrium and myometrium. It is mainly found on the surface of ovaries and pelvic peritoneum. The pouch of Douglas, uterosacral ligament, and torus uterinus are the most common pelvic sites of involvement [28]. The most common symptoms are dysmenorrhea, dyspareunia, irregular bleeding, and infertility, although a large percentage of patients are asymptomatic.

Laparoscopy is the gold standard for the diagnosis of endometriosis. However, MRI, as a non-invasive imaging modality, is increasingly being used to evaluate endometriosis that is located within the deep pelvis. MRI should be performed during the first 10 days of the menstrual cycle to better visualize small foci of bleeding. Ultrasound aids in evaluating the ovaries and in the general assessment of the pelvis in the workup for pelvic pain and infertility. There is variability in the ultrasound appearance of endometriomas. However, the classic appearance is a homogeneous lesion with low-level internal echoes. Unlike many other ovarian cysts, endometriomas do not resolve. On MRI, endometriomas typically appear as plaque-like lesions with or without hemorrhage and may have high T1 signal even with fat-suppression and variable T2 shading (Fig. 23).

Laparoscopic surgery can be performed for pain or infertility. Medical treatment targeting hormonal regulation can also be given for pain. Endometriosis is

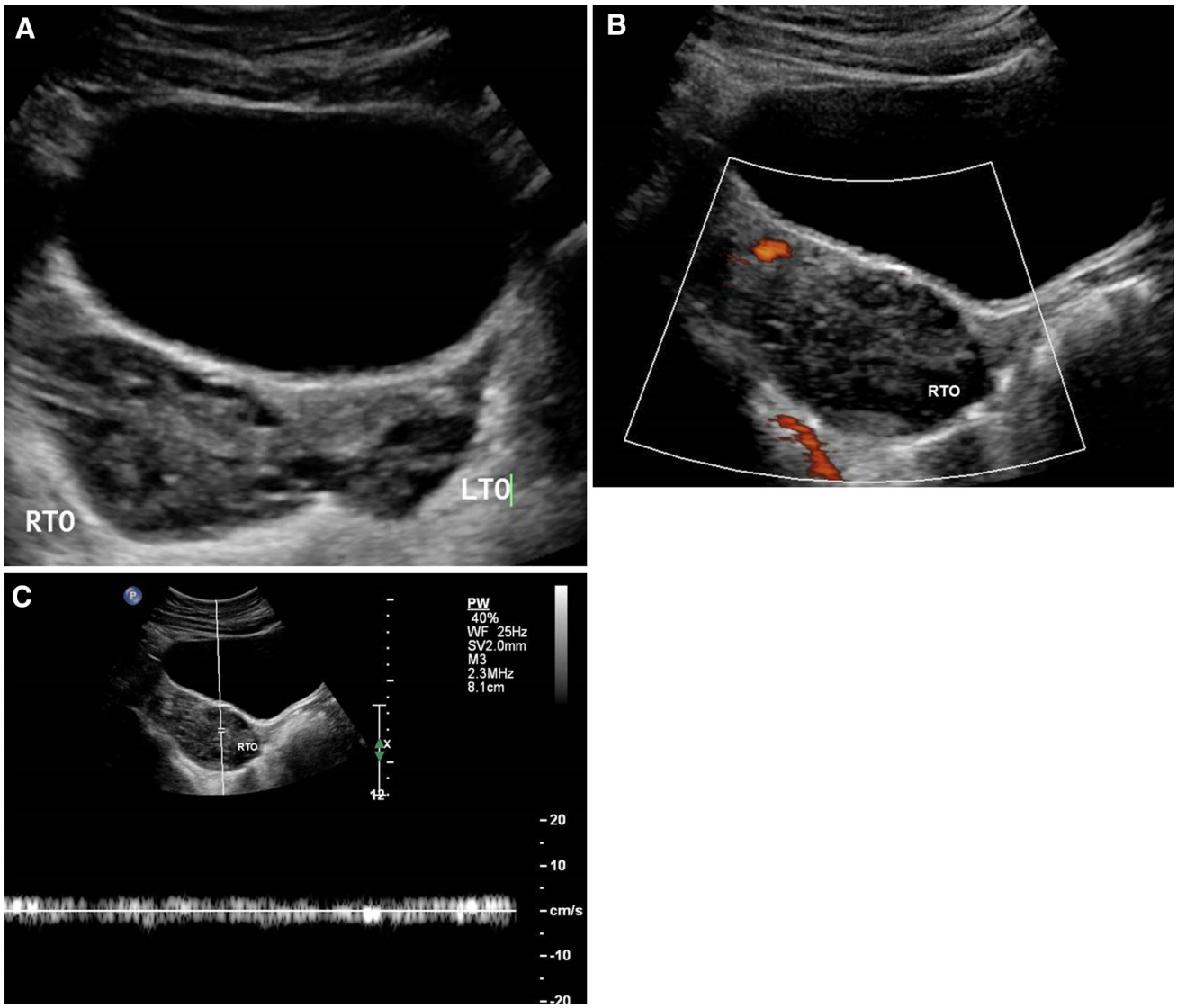

Fig. 22. Transverse grayscale ultrasound image through the pelvis (**A**) in a patient with abrupt onset of severe right lower quadrant pain demonstrates an asymmetrically enlarged right ovary (RTO) compared with the left ovary (LTO). Longitudinal ultrasound of the right adnexa with power Doppler (**B**) reveals no color flow within the right ovary (RTO). Spectral Doppler waveform from the right ovary (RTO) is shown to be abnormal with a lack of normal arterial flow (**C**). The constellation of ultrasound findings is consistent with ovarian torsion.

self-limiting in most affected pediatric patients generally improving with pregnancy or menopause. Malignant transformation can occur but is rare and is usually in the form of endometrioid carcinoma or clear cell carcinoma.

Conclusion

Right lower quadrant pain can be caused by various entities, from congenital to neoplastic conditions in the pediatric population. Clear knowledge of the spectrum of

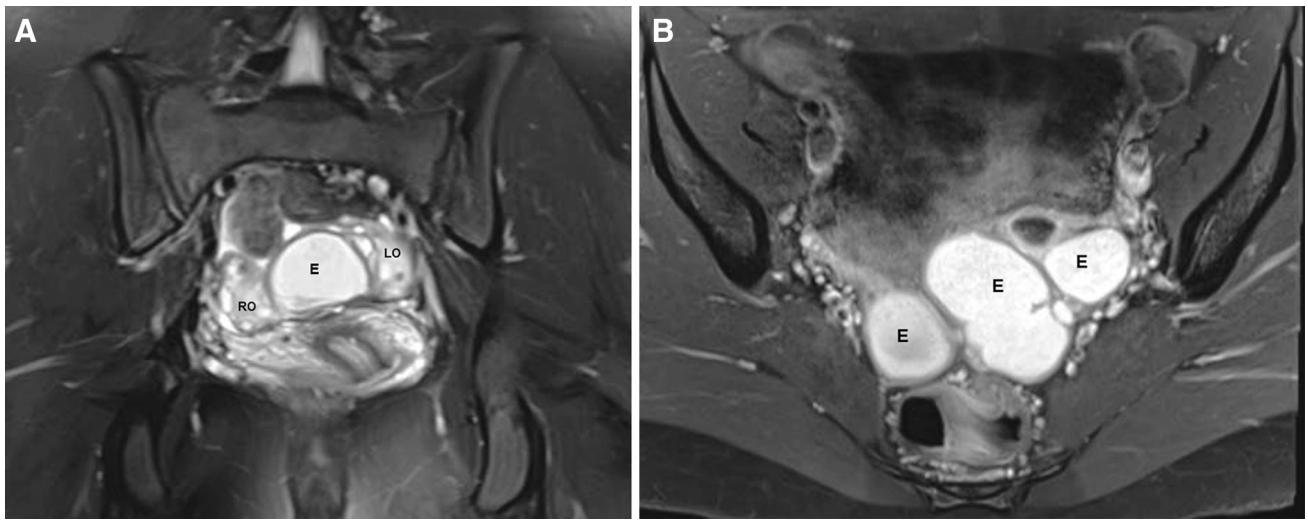

Fig. 23. Coronal T2 weighted MRI image with fat saturation (**A**) in an adolescent female with endometriosis reveals medialization of the right (RO) and left (LO) ovaries, which are adherent in the midline with an intervening T2 hyperintense structure (E). Axial T1 post-contrast fat-saturated image of the pelvis (**B**) reveals three T1 hyperintense masses (E) within the pelvis, just anterior to the rectum, consistent with endometriomas.

underlying causes is essential for the timely and appropriate management of pediatric patients, particularly those presenting with an acute surgical abdomen. Recognition of characteristic imaging features is important because it can guide treatment and may obviate unnecessary additional imaging studies or invasive procedures such as biopsy or surgery.

References

1. Manson D (2004) Contemporary imaging of the child with abdominal pain or distress. Paediatr Child Health 9(2):93–97
2. Rothrock SG, Green SM, Harding M, et al. (1991) Plain abdominal radiography in the detection of acute medical and surgical disease in children: a retrospective analysis. Pediatr Emerg Care 7(5):281–285
3. Mazzei MA, Guerrini S, Cioffi Squitieri N, et al. (2013) The role of US examination in the management of acute abdomen. Crit Ultrasound J 5(Suppl 1):S6. doi:10.1186/2036-7902-5-S1-S6
4. Strauss KJ, Goske MJ, Kaste SC, et al. (2010) Image gently: ten steps you can take to optimize image quality and lower CT dose for pediatric patients. AJR Am J Roentgenol 194(4):868–873. doi:10.2214/AJR.09.4091
5. Chavhan GB, Babyn PS, Singh M, Vidarsson L, Shroff M (2009) MR imaging at 3.0 T in children: technical differences, safety issues, and initial experience. Radiographics 29(5):1451–1466 (Review). doi:10.1148/rg.295095041
6. Chang KJ, Kamel IR, Macura KJ, Bluemke DA (2008) 3.0-T MR imaging of the abdomen: comparison with 1.5 T. Radiographics 28(7):1983–1998 (Review). doi:10.1148/rg.287075154
7. Anupindi S, Jaramillo D (2002) Pediatric magnetic resonance imaging techniques. Magn Reson Imaging Clin N Am 10(2):189–207
8. Pruessmann KP (2004) Parallel imaging at high field strength: synergies and joint potential. Top Magn Reson Imaging 15(4):237–244
9. Slovis TL (2011) Sedation and anesthesia issues in pediatric imaging. Pediatr Radiol 41(Suppl 2):514–516. doi:10.1007/s00247-011-2115-2
10. Cravero JP, Blike GT (2004) Pediatric sedation. Curr Opin Anaesthesiol 17(3):247–251
11. Rappaport B, Mellon RD, Simone A, Woodcock J (2011) Defining safe use of anesthesia in children. N Engl J Med 364(15):1387–1390. doi:10.1056/NEJMp1102155
12. Haliloglu M, Hoffer FA, Gronemeyer SA, Rao BN (1999) Applications of 3D contrast-enhanced MR angiograpy in pediatric oncology. Pediatr Radiol 29(11):863–868. doi:10.1007/s002470050714
13. Puligandla PS, Nguyen LT, St-Vil D, et al. (2003) Gastrointestinal duplications. J Pediatr Surg 38(5):740–744. doi:10.1016/jpsu.2003.50197
14. Blank G, Konigsrainer A, Sipos B, Ladurner R (2012) Adenocarcinoma arising in a cystic duplication of the small bowel: case report and review of literature. World J Surg Oncol 10:55. doi:10.1186/1477-7819-10-55
15. Orr MM, Edwards AJ (1975) Neoplastic change in duplications of the alimentary tract. Br J Surg 62(4):269–274
16. Levy AD, Hobbs CM (2004) From the archives of the AFIP. Meckel diverticulum: radiologic features with pathologic correlation. Radiographics 24(2):565–587 (Review). doi:10.1148/rg.242035187
17. Bani-Hani KE, Shatnawi NJ (2004) Meckel's diverticulum: comparison of incidental and symptomatic cases. World J Surg 28(9):917–920
18. Ashley RA, Inman BA, Routh JC, et al. (2007) Urachal anomalies: a longitudinal study of urachal remnants in children and adults. J Urol 178(4 Pt 2):1615–1618. doi:10.1016/j.juro.2007.03.194
19. Navarro O, Daneman A (2004) Intussusception. Part 3: diagnosis and management of those with an identifiable or predisposing cause and those that reduce spontaneously. Pediatr Radiol 34(4):305–312 (quiz 369). doi:10.1007/s00247-003-1028-0
20. Ein SH (1976) Leading points in childhood intussusception. J Pediatr Surg 11(2):209–211
21. Pritt BS, Clark CG (2008) Amebiasis. Mayo Clin Proc 83(10):1154–1159 (quiz 1159–1160). doi:10.4065/83.10.1154
22. Wilhelmi I, Roman E, Sanchez-Fauquier A (2003) Viruses causing gastroenteritis. Clin Microbiol Infect 9(4):247–262 (Review)
23. Sauer CG, Kugathasan S (2009) Pediatric inflammatory bowel disease: highlighting pediatric differences in IBD. Gastroenterol Clin North Am 38(4):611–628. doi:10.1016/j.gtc.2009.07.010
24. Grattan-Smith JD, Blews DE, Brand T (2002) Omental infarction in pediatric patients: sonographic and CT findings. AJR Am J Roentgenol 178(6):1537–1539. doi:10.2214/ajr.178.6.1781537
25. Ting TV, Hashkes PJ (2004) Update on childhood vasculitides. Curr Opin Rheumatol 16(5):560–565
26. Karlo CA, Gnannt R, Winklehner A, et al. (2013) Split-bolus dual-energy CT urography: protocol optimization and diagnostic performance for the detection of urinary stones. Abdom Imaging 38(5):1136–1143. doi:10.1007/s00261-013-9992-9

27. Ascenti G, Siragusa C, Racchiusa S, et al. (2010) Stone-targeted dual-energy CT: a new diagnostic approach to urinary calculosis. AJR Am J Roentgenol 195(4):953–958. doi:10.2214/AJR.09.3635

28. Kinkel K, Chapron C, Balleyguier C, et al. (1999) Magnetic resonance imaging characteristics of deep endometriosis. Hum Reprod 14(4):1080–1086